

氮掺杂还原氧化石墨烯与吡啶共聚 g-C₃N₄ 复合光催化剂及其增强的产氢活性

程若霖^{1,2} 金锡雄^{1,2} 樊向前^{1,2} 王敏^{1,2} 田建建^{1,2}
张玲霞^{1,2,*} 施剑林^{1,2,*}

(¹中国科学院上海硅酸盐研究所, 高性能陶瓷和超微结构国家重点实验室, 上海 200050; ²中国科学院大学, 北京 100049)

Incorporation of N-Doped Reduced Graphene Oxide into Pyridine-Copolymerized g-C₃N₄ for Greatly Enhanced H₂ Photocatalytic Evolution

CHENG Ruo-Lin^{1,2} JIN Xi-Xiong^{1,2} FAN Xiang-Qian^{1,2} WANG Min^{1,2}
TIAN Jian-Jian^{1,2} ZHANG Ling-Xia^{1,2,*} SHI Jian-Lin^{1,2,*}

(¹State Key Laboratory of High Performance Ceramics and Superfine Microstructure, Shanghai Institute of Ceramics, Chinese Academy of Sciences, Shanghai 200050, P. R. China; ²University of Chinese Academy of Sciences, Beijing 100049, P. R. China)

*Corresponding authors. SHI Jian-Lin, Email: jlshi@mail.sic.ac.cn; Tel: +86-21-52412706.

ZHANG Ling-Xia, Email: zhlingxia@mail.sic.ac.cn; Tel: +86-21-52412706.

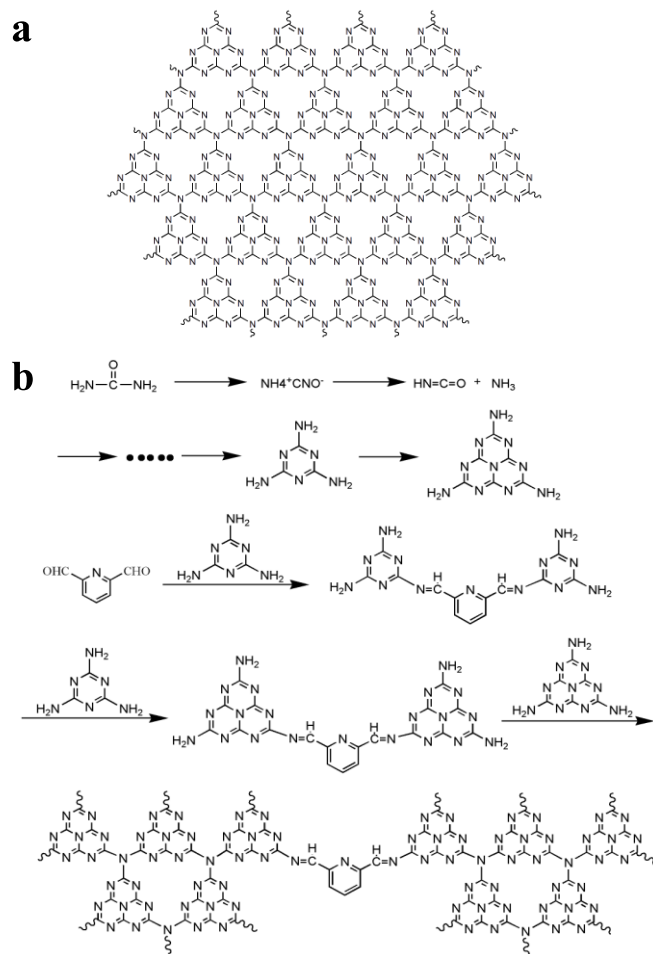


Fig.S1 (a) Possible reaction path of incorporating pyridine into g-C₃N₄ networks¹, (b) the structure of g-C₃N₄.

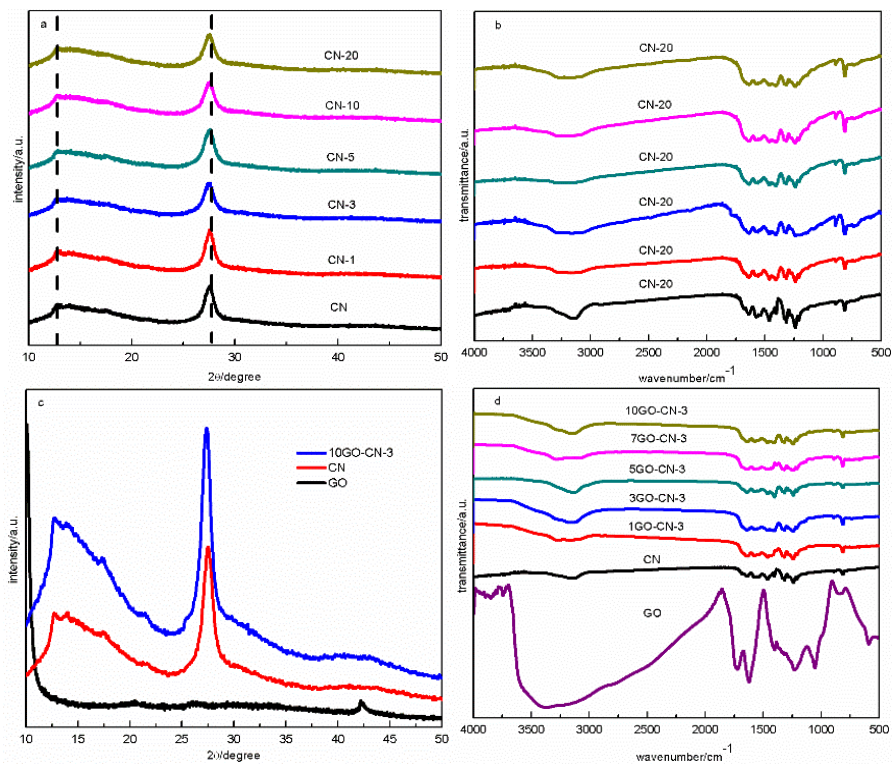


Fig.S2 XRD patterns (a) (c) and FT-IR spectra (b) (d) of CN, GO, CN-x and yGO-CN-3.

In Fig.S2a, the distinct peak at 27.48° belongs to the characteristic (002) interlayer-stacking reflection of aromatic system, and the other pronounced peak at 12.78° originates from (100) plane and represents the in-plane structural packing motif². In Fig.S2b, a series of strong bands at $1200\text{--}1650\text{ cm}^{-1}$ originate from the typical stretching modes of 3, s-triazine heterocyclic (C_6N_7) rings. The broad bands at about $3000\text{--}3500\text{ cm}^{-1}$ correspond to the adsorbed H_2O molecules and the terminal amino groups in g- C_3N_4 . The most intense band located at 809 cm^{-1} represents the out-of-plane bending vibration of 3, s-triazine rings. In the composite 10GO-CN-3 (Fig.S2c), only the characteristic peaks of g- C_3N_4 can be observed, indicating the well-crystallized structure of g- C_3N_4 has been well retained. For GO (Fig.S2d), the characteristic band at 854 cm^{-1} is attributed to epoxide groups. The peaks at 1406 , 1220 and 1053 cm^{-1} correspond to $-\text{OH}$, $\text{C}-\text{OH}$ and $\text{C}-\text{O}-\text{C}$ groups, respectively.

Table S1 Elemental composition and C/N molar ratio of CN, CN-x and yCN-3.

Sample	w/%			C/N mass ratio
	C	N	H	
CN	34.600	57.720	1.705	0.6994
CN-1	34.585	57.980	1.709	0.6959
CN-3	34.865	57.970	1.714	0.7017
CN-5	34.840	57.790	1.742	0.7034
CN-10	34.745	57.445	1.758	0.7056
CN-20	34.755	57.140	1.769	0.7096
1GO-CN-3	34.745	58.105	1.675	0.6976
3GO-CN-3	34.835	58.055	1.660	0.7000
5GO-CN-3	34.460	57.335	1.803	0.7012
7GO-CN-3	34.515	57.170	1.786	0.7043
10GO-CN-3	34.855	57.745	1.671	0.7042

Table S2 Summary of surface area and bandgap results of the as-prepared samples

Sample	$S_{\text{BET}}/(\text{m}^2\text{ g}^{-1})$	Bandgap/eV
CN	80	2.94
CN-1	83	2.93
CN-3	82	2.87
CN-5	78	2.83
CN-10	75	2.83
CN-20	73	2.75
1GO-CN-3	92	2.87
3GO-CN-3	97	2.86
5GO-CN-3	95	2.85
7GO-CN-3	107	2.82
10GO-CN-3	99	2.80

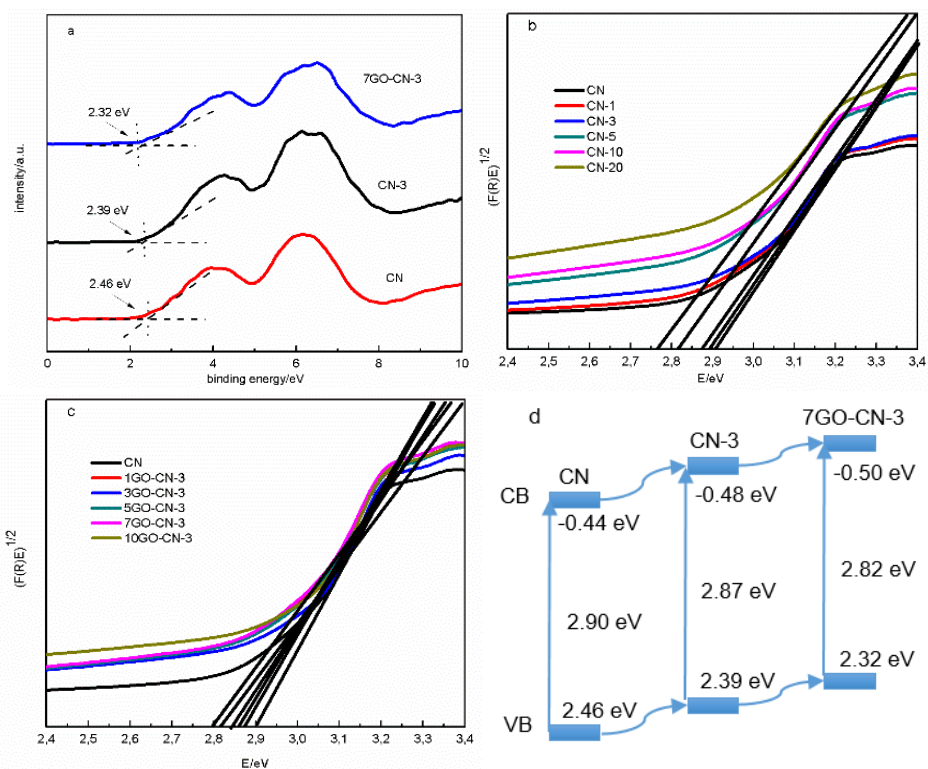


Fig.S3 (a) Valence band XPS spectra of traditional CN, CN-x and yGO-CN-3; The Tauc plots of (b) CN and CN-x samples, (c) CN and yGO-CN-3, each band gap is determined by the intersection point of the corresponding dashed tangent line and the horizontal axis; Schematic of the relative positions of HOMO and LUMO energy levels for CN, CN-3 and 7GO-CN-3.

References

- (1) Fan, X. Q.; Zhang, L. X.; Wang, M.; Huang, W. M.; Zhou, Y. J.; Li, M. L.; Cheng, R. L.; Shi, J. L. *Appl. Catal. B: Environ.* **2016**, *182*, 68. doi: 10.1016/j.apcatb.2015.09.006
- (2) Cui, Y. J.; Zhang, J. S.; Zhang, G. G.; Huang, J. H.; Liu, P.; Antonietti, M.; Wang, X. C. *J Mater. Chem.* **2011**, *21*, 13032. doi: 10.1039/c1jm11961c